

## SELFCONSTRICTING DISCHARGES IN DEUTERIUM AT HIGH RATES OF CURRENT GROWTH

V. S. KOMEL' KOV

Submitted to JETP editor February 6, 1958

J. Exptl. Theoret. Phys. (U.S.S.R.) **35**, 16-26 (July, 1958)

Results of investigation of selfconstricting discharges are described for rates of current rise in the range  $7 \times 10^{11}$  to  $1.4 \times 10^{12}$  amp/sec, and for current amplitudes up to  $2 \times 10^6$  amp. The initial deuterium pressure in the chambers varied between 0.1 and 10 mm of Hg. The highest gas temperature that was possibly attained was about 200 ev.

### 1. INTRODUCTION

IN earlier papers<sup>1-3</sup> a description was given of the development of a powerful electric discharge in deuterium at pressures between  $10^{-3}$  and 1 mm of Hg. Basic quantitative relations which agreed in a satisfactory manner with the experimental data, were also given. All the investigations referred to above were carried out with the aid of apparatus which made it possible to attain an initial rate of current rise of  $5 \times 10^{10}$  to  $1.5 \times 10^{11}$  amp/sec. Since an increase in the initial rate of current rise was accompanied by an increase in the velocities and the temperature of the gas at the instant of complete contraction, it appeared to be of interest to investigate these processes at the highest attainable rates and amplitudes of the current.

With reference to the capacitor installation which was at our disposal, an increase in these parameters was possible only by decreasing the inductance of all the elements of the circuit (capacitors, current leads, discharge gap), and also by decreasing the inductance of the discharge column itself. The methods which were used to decrease the inductances of the circuit have been described by Komel'kov and Aretov.<sup>4</sup> In order to reduce the inductance of the discharge column it was necessary to reduce the height of the chamber to a few centimeters, and to limit the range of the initial gas pressure in the chamber from 0.1 to 10 mm of Hg. If the gas pressure is reduced further, the vapor of the metal of the electrodes fills the working volume of the chamber too rapidly and cools the gas.

To obtain photographic records, use was made of transparent glass chambers with flat metallic electrodes. The energy liberated by the circuit during the discharge was so great that the cham-

ber was repeatedly completely destroyed. Under such conditions, probe measurements, which require averaging over many experiments, would have made the experiment very complicated. They had to be discarded, and we had to limit ourselves only to optical recording of the constriction, and to recording the current and the voltage across the chamber electrodes. The experiments described below have been carried out with the participation of D. S. Parfenov, G. N. Aretov, and B. P. Surnin.

### 2. THE TECHNIQUE AND THE EXPERIMENTAL METHOD

1. The discharge under investigation took place in glass chambers of 190 mm internal diameter. The height of the chamber, the form of the electrodes, the discharge gap, and the current lead connections are shown in the figures given below. In order to prevent the breakdown of the short chambers along the surface of the wall (in air) the rubber insulation of the circuit was introduced inside the chamber, and served at the same time as a vacuum seal. The mechanical strength of the conductors in the immediate vicinity of the chamber was increased by means of steel braces. Because of this, the conductors lasted through the whole series of experiments without undergoing any appreciable deformation. The air was pumped out of the chamber by an oil diffusion pump down to a pressure of  $10^{-5}$  mm of Hg. The chamber was filled with 98.9% pure deuterium through an opening in the lower electrode.

2. The electric circuit diagram of the apparatus is given in Fig. 1. The capacitance  $C_1$  of the main capacitor bank was 130  $\mu$ f. An auxiliary capacitor  $C_2 = 3 \mu$ f was connected in parallel with it. Both capacitors were charged through a

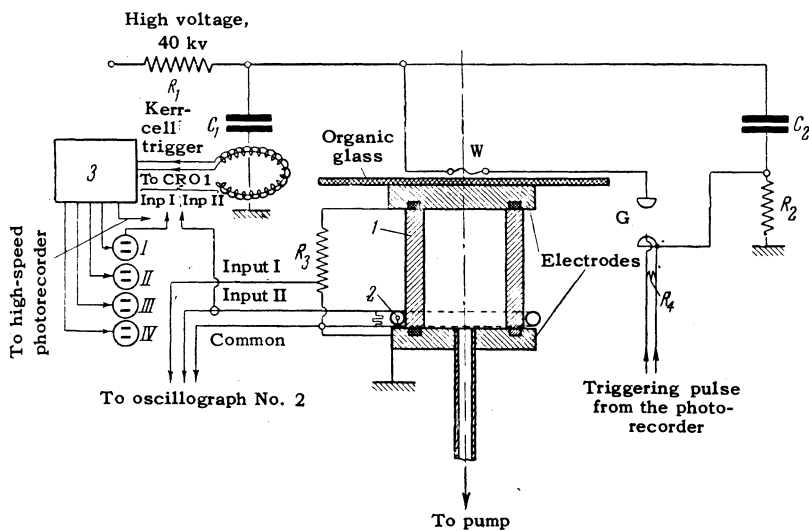


FIG. 1. Electrical circuit diagram of the apparatus. 1 – glass chamber; 2 – Rogovskii belt; 3 – control unit for the Kerr cells; I, II, III, IV – Kerr cells.

resistance  $R_1 = 300 \text{ k}\Omega$  until they reached equal potential. Variations in the diameter of the discharge channel were recorded by means of a fast mirror photorecorder SFR-2M. When the mirror was in the working position, the photo-recorder sent a triggering pulse to the discharging air gap G. The capacitor  $C_2$  was discharged into a grid of thin wires W which exploded as a result of this, and broke the thin (1 to 2 mm thickness) insulation made of organic glass. The discharge of the main capacitor  $C_1$  into the chamber occurred from 2 to  $10 \mu\text{sec}$  after the triggering pulse. The resistance  $R_2 = 10^6 \Omega$  is introduced into the circuit in order to limit the discharge current to ground after the breakdown of the discharge gap G. The ohmic potential divider was made of a bifilar wound resistor ( $R_3 = 810 \Omega$ ) connected to the chamber electrodes. The potential divider was situated outside the current conductors, where there were no magnetic fields. The connecting conductor leading to the upper electrode passed through the main conductors; the inductance of the loop formed by it was not larger than 2 cm. The voltage at the output of the potential divider amounted to 0.01 of the circuit voltage. The discharge current (measured by means of a Rogovskii belt) and the voltage on the potential divider were recorded by a double beam oscillograph OK-17M.

Simultaneously with the photo-scanning, the discharge was photographed by means of four Kerr cells which were fed with 15-kv pulses from a special unit which was switched on at the start of the discharge of capacitor  $C_1$ . This unit generated five pulses; four reached the Kerr cells, and one reached the spark gap of the photorecorder, producing a light marker on the film. This marker (cf. the "Synchr" marker in Figs.

3 to 5 and 10) enabled us to establish the correspondence between the current oscillograms and the photographic records. To reduce the background on the records given by the Kerr cells, explosive shutters were installed near the observation window of the chamber container.

### 3. EXPERIMENTAL RESULTS

(a) **Small Chamber.** The construction of the chamber is shown in Fig. 2. The chamber was situated inside a depression of the lower current conductor, covered by a reinforced top. The period of current oscillations during the discharge of the capacitor bank into the chamber was  $12.2 \mu\text{sec}$ . The inductance of the whole circuit, calculated from the second and the third periods of the current, did not exceed 27.5 cm.\* On the basis of measurements and calculations the inductances of the individual circuit elements have the following values: (1) The inductance of the capacitor bank is 6.5 cm; (2) the inductance of the current lead is 6.0 cm; (3) the inductance of the discharge gap (over one period) is 8.5 cm; (4) the inductance of the chamber together with the flanges is 6.5 cm. The maximum rate of current growth in the circuit with a working voltage of  $U_0 = 40 \text{ kv}$  reached a value of  $1.4 \times 10^{12} \text{ amp/sec}$ . The measured amplitude of the current in the circuit amounted to  $1.8 \times 10^6 \text{ amp}$ . The current graph in the case of discharge through short chambers has rather insignificant variations during the contraction and the expansion of the discharge channel. This may be explained by the fact that the inductance of the constricted discharge channel amounts to not more than  $\frac{1}{3}$  of the inductance of the whole circuit.

\*1 cm =  $10^{-9}$  henry – Transl. Ed.

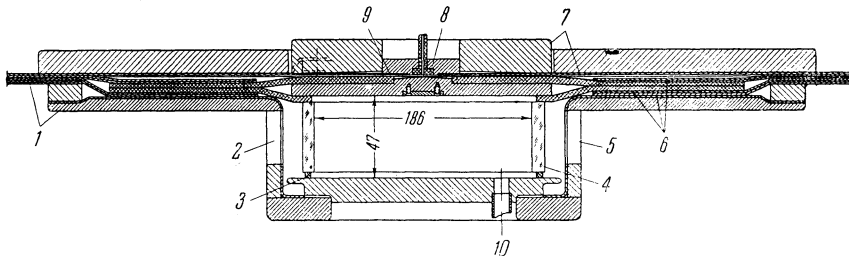


FIG. 2. Construction of the small chamber. 1 – grounded conductor; 2 – window for photographing the discharge by means of Kerr cells; 3 – rubber seal; 4 – glass chamber; 5 – window for photographing the discharge by means of the photorecorder; 6 – rubber insulation; 7 – high voltage conductor; 8 – explosive discharger; 9 – organic glass; 10 – to vacuum pump.

At a pressure of 10 mm of Hg the discharge and the luminescence of the gas at first take place over the whole volume, and then the luminescence becomes weaker. After a pause of  $0.6 \mu\text{sec}$ , it again becomes more intense near the chamber walls. As many as 30 narrow channels are formed which are relatively more luminous and which gradually expand. Their approach towards one another forms, in fact, the constriction of the discharge which proceeds at an ever increasing rate. During the initial period of constriction, the speed is not greater than  $1.5 \times 10^6 \text{ cm/sec}$ , but at the instant of maximum constriction it amounts to  $5.4 \times 10^6 \text{ cm/sec}$ . Figure 3 shows the photorecorder display, the Kerr-cell records, and the oscillograms of the current and of the voltage for this discharge. We see that a constriction has formed in the middle of the channel, just at the point where the photorecorder slit is situated. At this spot the maximum speed of the gas referred to earlier exceeds the average speed of contraction of the channel by a factor of 2.7. Complete contraction occurs near the maximum of the current which is equal to  $1.38 \times 10^6 \text{ amp}$ . At this instant a characteristic break occurs in the current curve, called a "singularity" in the papers referred to earlier. The minimum radius of the constricted channel is equal to 1.7 cm. The expansion of the gas after the constriction occurs with an initial speed of  $3.6 \times 10^6 \text{ cm/sec}$ . The speed of expansion gradually decreases. During the sixth microsecond a second constriction begins, but does not have time to be completed, since a part of the gas reaches the wall causing its evaporation and the formation of a new wave containing a large admixture of the material of the wall. Therefore repeated waves coming from the wall (not shown in the photograph) approach the center considerably more slowly. The boundaries of the channel are quite sharply pronounced during the first contraction, and the luminescence of the walls is not very noticeable at that time. As soon as the converging layers of the gas meet one another, the walls of the chamber begin to emit light, apparently owing to the

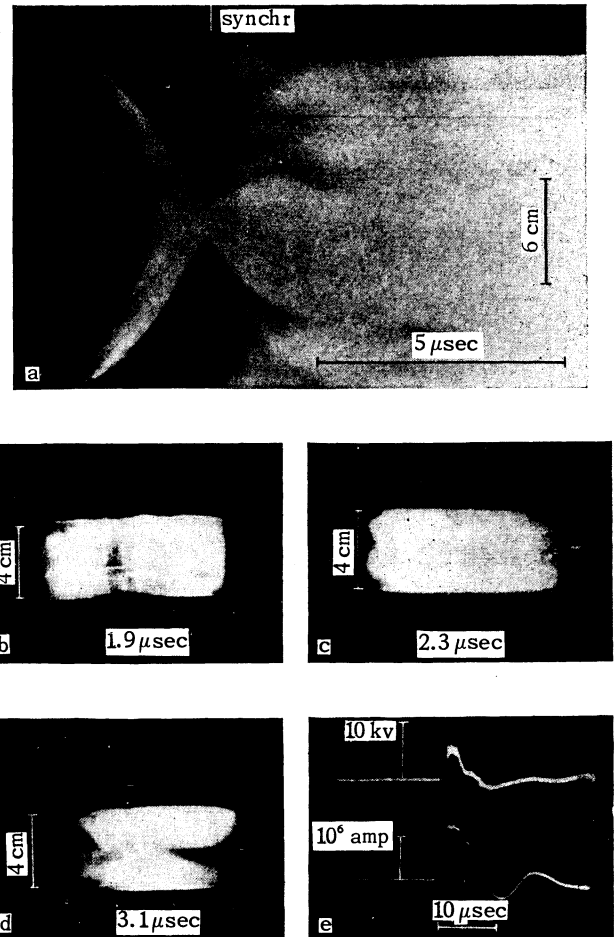


FIG. 3 a – photorecorder display, b, c, d – Kerr-cell records, e – current and voltage oscillograms for discharges in small chambers at a pressure of 10 mm of Hg.

short-wave radiation from the discharge channel. The luminescence of the walls is not accompanied by any breakdown or redistribution of current, since otherwise this would have been made evident by the photorecorder display.

During the initial contraction period, the current in the discharge is equal to 620 kiloamp. If this is evaluated for the individual channels that can be seen on the photorecorder display, then the average current in each channel is approximately 20 kiloamp. After a microsecond it reaches 440 to

550 kiloamp. Simultaneously with their movement towards the center, the channels expand with a speed of  $(0.8 \text{ to } 1.0) \times 10^6 \text{ cm/sec}$ . The channels merge into a continuous annular layer during the third microsecond. The thickness of this layer obtained as a result of measurements made on the photorecorder display is 3 cm.

The intensity of the field in the discharge was calculated from the oscillograms, using the relations:

$$E_R = \frac{U_R}{l}; \quad U_R = U_0 - L \frac{dI}{dt} - I \frac{dL}{dt},$$

where  $U_0$  is the voltage recorded on the oscillogram,  $L$  the inductance of the loop formed by the measuring wire (leading to the upper electrode) and the discharge channel,  $l$  the distance between the electrodes, and  $I$  the current in the discharge.

At the beginning of the contraction ( $dL/dt = 0$ ).  $E_R = 850 \text{ v/cm}$ . Subsequent measurements of  $E_R$  become unreliable, owing to oscillations which make it difficult to determine the derivative of the current.

At a pressure of 1 mm of Hg, the discharge emits considerably less light. The constriction process has much in common with the one described earlier. Just as in the earlier case, the expansion of the gas differs appreciably from a simple motion of shock waves (cf. Fig. 4). The luminous layer of gas begins to move towards the center of the chamber after the discharge current has reached 550 kiloamp. This layer consists of 30 small channels whose brightness considerably exceeds the brightness of luminescence of the surrounding gas. As the channels move towards the center of the chamber, they practically do not expand. The internal boundaries of the layer undergoing contraction touch one another  $1.5 \mu\text{sec}$  after the beginning of the discharge. The thickness of the layer at that instant amounts to 2.2 cm. The speed of contraction is initially equal to  $4.5 \times 10^6 \text{ cm/sec}$ . By the time of complete contraction, it reaches a value of  $8 \times 10^6 \text{ cm/sec}$ . The minimum radius of the column is 1.5 cm. The current at the "singularity" is  $1.6 \times 10^6 \text{ amp}$  at the instant of constriction. The external regions of the gas being compressed approach the center  $0.3 \mu\text{sec}$  later, and restrain the expansion of the gas whose speed at that time does not exceed  $1.5 \times 10^6 \text{ cm/sec}$ . After the outer layers have approached, the speed of expansion increases to  $9 \times 10^6 \text{ cm/sec}$ . Cylindrical symmetry of the column of the contracting gas is retained both before and after expansion. Soon after the beginning of the expansion the gas separates into layers. One part goes back

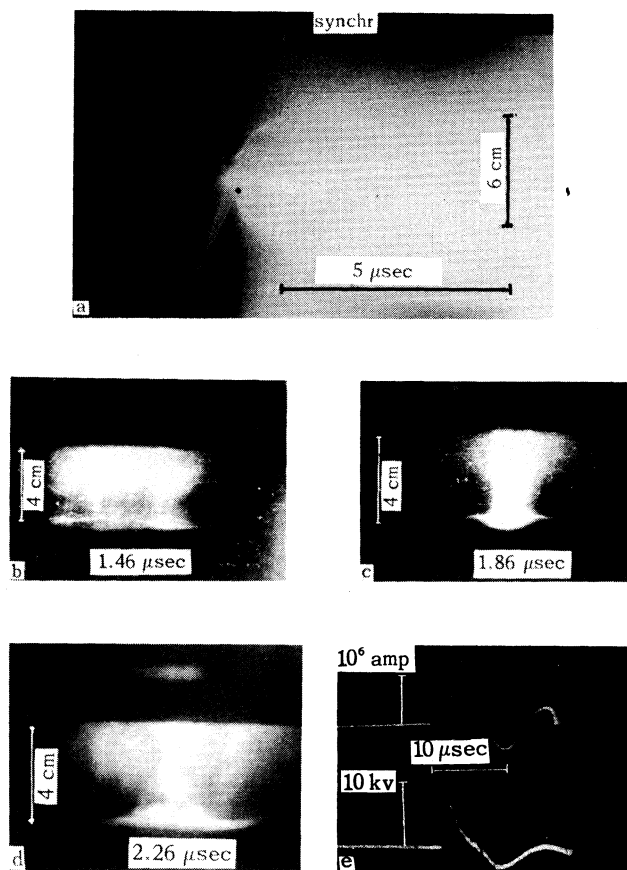


FIG. 4 a – photorecorder display, b, c, d – Kerr-cell records, e – current and voltage oscillograms for discharges in small chambers at a pressure of 1 mm of Hg.

towards the center of the chamber where the luminous channel remains, and another part of the gas goes towards the chamber walls.

The stratification occurs three times separated by intervals of  $0.2 \text{ to } 1 \mu\text{sec}$  and, apparently, is of a symmetric nature, as may be seen from the third Kerr-cell record. The internal column is more brightly luminous, and may be picked out in the photograph right up to the fourth microsecond. Small oscillations in the oscillograms of the current and the voltage, which last right up to the fifth microsecond, correspond to the fluctuations in the gas column.

At a pressure of 0.1 mm, the relative luminosity of the chamber walls increases, and this makes it more difficult to interpret the photograph. Nevertheless the principal features can still be seen (Fig. 5). A characteristic feature of the process is the occurrence not of one, but of three compression waves moving towards the center with constant velocity at times equal to  $0.44$ ,  $0.85$ , and  $1.46 \mu\text{sec}$  after the beginning of the compression. The velocities of the fronts amount respectively to  $8.6 \times 10^6$ ,  $1.1 \times 10^7$ , and  $1.4 \times 10^7 \text{ cm/sec}$ . The second and

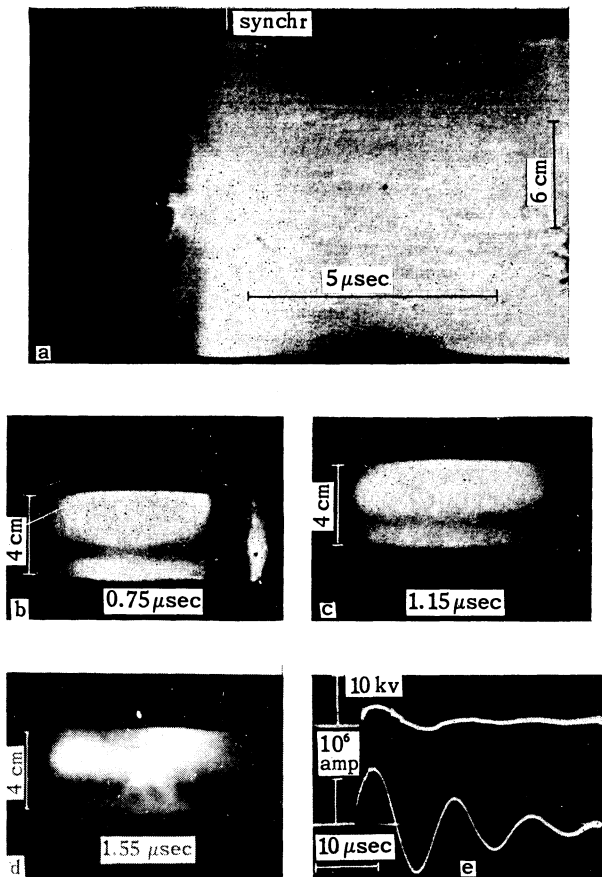


FIG. 5 a – photorecorder display, b, c, d – Ker-cell records, e – current and voltage oscillograms for discharges in small chambers at a pressure of 0.1 mm of Hg.

the third fronts begin to move even before the preceding front has reached the center of the chamber. The individual channels in these fronts appear not at the beginning, but almost at the time of complete contraction. The channels approach one another, forming constrictions of a certain kind, which shows that the currents flowing in them are parallel.

Both in the photorecorder displays and also in the Kerr-cell records (the two are in good agreement) it can be noted that the channels are surrounded by an atmosphere of luminous gas within which they approach one another. The separation begins after the first compression and slows down as each successive front approaches the center of the chamber. The minimum diameter of the channel is 1.5 cm during the first contraction, 3.7 cm during the second, and 5.6 cm during the third. The total current in the circuit, at the instant when the first wave starts, amounts to 350 kiloamp; for the second and third waves this current is respectively 900 and 1200 kiloamp. To each compression there correspond small oscillations in the oscillogram of the current whose maximum values for each of the waves are  $1.1 \times 10^6$ ,  $1.2 \times$

$10^6$  and  $1.3 \times 10^6$  amp. In view of the fact that the compression waves are superimposed in time, the measured current can be related to the discharge column only for the third wave.

The voltage across the electrodes, as recorded by the oscillograph, at first falls and then rises; during the first microsecond it amounts to 4300 v, it then increases to 14.4 kv and remains at this level until the fourth microsecond. The gradient in the chamber when the current through it passes through its maximum (when there is no inductive component) is 3 kv/cm. At pressures of 10 and 1 mm of Hg, a falling off of the voltage was observed during the first and second microseconds.

(b) **Large Chamber.** Just as in the preceding case, in the case of experiments with the large chamber an explosive discharger was used, placed between the upper flat flange of the chamber and the high-voltage lead. The lower flange had a small convex portion which was made in order to introduce the head of a scintillation counter into the depression that is formed below. The height of the glass chamber was 155 mm. The distance between the projection in the lower electrode and the upper electrode was 123 mm, the inner radius of the chamber was 92 mm. The small convex projection of the lower electrode did not affect the process of constriction which proceeded in exactly the same manner as in the case of a flat lower electrode. The copper conductor surrounding the chamber had a flare in its lower part. On top, a steel ring was placed around the copper coaxial cable to increase its mechanical strength. The total inductance of the circuit together with the chamber and the discharger, as evaluated from the period of oscillations of the current, did not exceed 55 cm. The inductance of the measuring loop at the beginning of the process (when the current flows near the chamber walls) attained a value of 7 cm. The initial rate of rise of the current in the discharge was  $0.73 \times 10^{12}$  amp/sec.

At a pressure of 10 mm of Hg the contraction process begins already at a current of 500 to 600 kiloamp after a number of narrow channels (approximately 40) have been formed in the discharge. The contraction takes place with an average speed of  $3 \times 10^6$  cm/sec (cf. Fig. 6). The converging layer of gas had a thickness of 2.5 to 3 cm. The inner boundaries of the layer met  $3.2 \mu$  sec after the start, the outer ones met  $0.6 \mu$  sec later. At the instant of complete contraction when the diameter of the channel was reduced to 3.6 cm the current in the discharge attained a value of  $1.1 \times 10^6$  amp, and owing to the relative increase in the inductance of the discharge channel the current

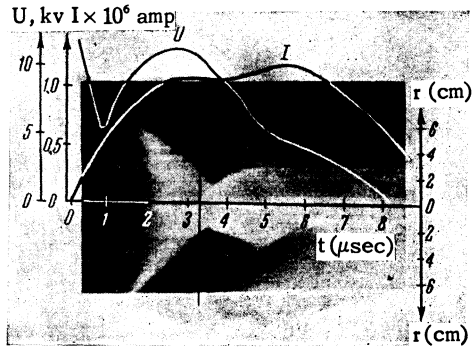


FIG. 6. Photorecorder display of a discharge at  $p = 10$  mm. of Hg with the current and voltage oscillograms superimposed on it.

lost its sinusoidal form. The peak of the sinusoidal curve was flattened and showed dips characteristic of the so-called "singularities." The expansion of the gas occurs with speeds in the range  $(1.2 \text{ to } 2.1) \times 10^6$  cm/sec. A second compression was observed 1.5 microsec after the first one; the diameter of the channel in this case was reduced to 7 cm. The current at the second "singularity" was larger than at the first by 100 kiloamp. Between the instant of breakdown and the beginning of the compression, the voltage across the electrodes fell from 40 to 5.5 kv, and then increased to 12 kv. The maximum of the voltage coincides with the beginning of the "singularity" on the current curve, and is delayed with respect to the moment of complete contraction which may be seen on the photorecorder display.

At a pressure of 1 mm of Hg, the contraction begins 1.16  $\mu$  sec after breakdown. The speed of contraction varies between  $4.8 \times 10^6$  and  $6.1 \times 10^6$  cm/sec. In the photorecorder display (Fig. 7) one may see, just as in the preceding cases, a network of channels forming the contracting layer; the thick-

ness of the latter is 2.2 cm. On the Kerr-cell records horizontal bands can be seen which are particularly noticeable at times immediately preceding a complete contraction. Their appearance indicates that the instability characteristic of the plasma manifests itself in the contracting layer even before complete contraction has taken place. Complete contraction occurs 2.7  $\mu$  sec after breakdown and lasts 0.3  $\mu$  sec. The minimum diameter of the constricted channel is 1.7 cm. The expansion of the gas occurs in an asymmetrical manner: the channel remains constricted at the electrodes for some time, while at other points the expansion occurs more rapidly. The speed of expansion attains values up to  $3.7 \times 10^6$  cm/sec. A second compression begins 0.25  $\mu$  sec later, and takes place with a speed of  $4.5 \times 10^6$  cm/sec; then a small expansion occurs, and after that the diameter of the channel practically does not change until the sixth microsecond. Thus the channel remains constricted during 3 to 4 microsec.

The current in the discharge varied in the following way: at the moment when the gas separated from the walls its value was  $I_0 = 576$  kiloamp. During the first compression it was  $1.16 \times 10^6$  amp, and during the second compression it was  $1.3 \times 10^6$  amp.

(c) Chamber with conical electrodes. The construction of the chamber is shown in Fig. 8. The upper convex electrode has the form of a truncated cone with its vertex directed into the chamber. The lower electrode is the same as in the preceding chamber. With this construction of the electrodes, in spite of the small gap at the center of the chamber, the discharge is formed at the chamber walls. To make it easier for the breakdown to occur at the center, in some of the experiments sharp points were placed on the flat summit of the upper elec-

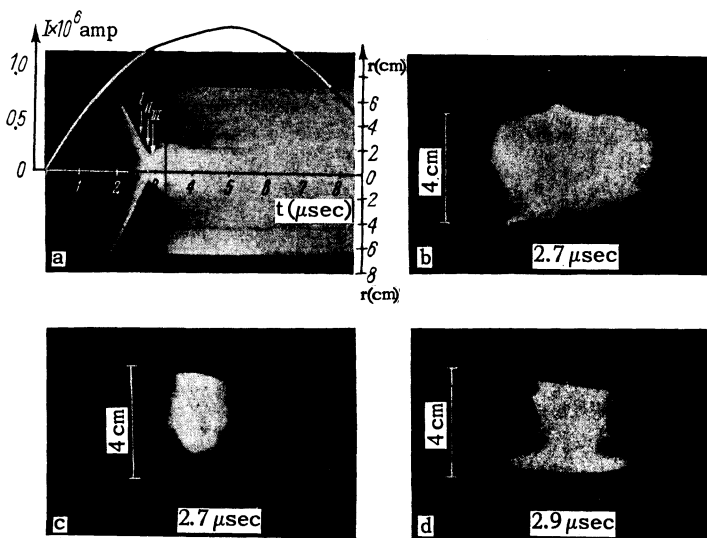


FIG. 7. a - photorecorder display with current oscillogram superimposed on it; b, c, d - Kerr-cell records of the discharge at a pressure of 1 mm of Hg.

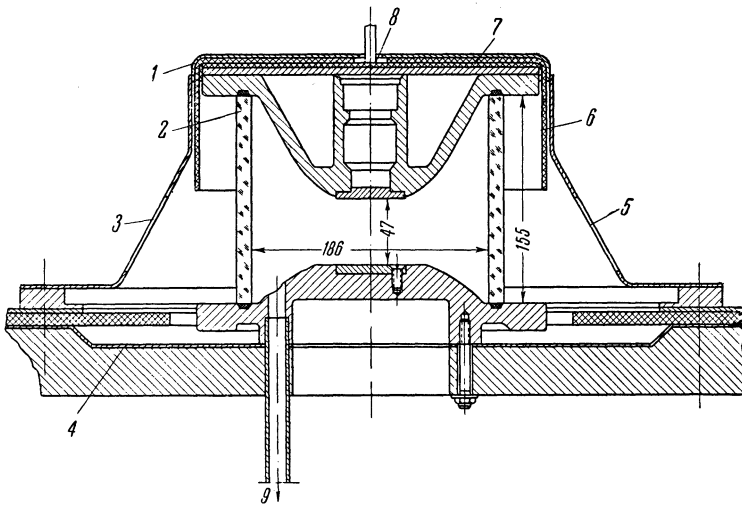


FIG. 8. Construction of chamber with conical electrodes. 1 – high voltage conductor, 2 – glass chamber, 3 – window for photographing the discharge by means of Kerr-cells, 4 – grounded conductor, 5 – window for photographing the discharge by means of photorecorders, 6 – rubber, 7 – organic glass, 8 – explosive discharger, 9 – to vacuum pump.

trode in such a way that the minimum gap between the electrodes was reduced to 17 mm.

At a pressure of 10 mm of Hg, the upper electrode was provided with a sharp point, but this did not prevent the formation of a skin-layer near the walls of the chamber. Although breakdowns were sometimes observed in the center of the chamber, nevertheless the main part of the current apparently flowed near the walls. The phenomenological aspects of the phenomena remained the same as in the preceding cases (Fig. 9). The start occurred 0.5 to 0.7  $\mu$ sec after breakdown. The speed of contraction at the beginning amounted to  $1.3 \times 10^6$  cm/sec, and then increased to  $5.2 \times 10^6$  cm/sec. The diameter of the channel was reduced from 18.5 to 2.3 cm. The expansion of the channel occurs in a fairly symmetric manner with a speed of  $5 \times 10^6$  cm/sec. Repeated contractions in these experiments are more sharply defined, they occur 1  $\mu$ sec and 2.5  $\mu$ sec after the first contraction.

At a pressure of 1 mm of Hg, the sharp point was removed from the upper electrode. The skin layer is formed at the wall and begins to contract 0.6  $\mu$ sec after breakdown with the total current in the discharge having a value of 370 kiloamp (Fig. 10). The initial speed of contraction is  $2.8 \times 10^6$  cm/sec, and the final speed is  $7.8 \times 10^6$  cm/sec. Just as in the two preceding cases contraction proceeds at this pressure quite symmetrically. The photographs by means of the Kerr cells allow us to observe in the gas layer various forms of instability which manifests itself practically from the very beginning. At the moment of complete contraction they are transformed into the "constrictions" described above. The contraction of the skin layer lasts not longer than 0.3  $\mu$ sec, after which expansion begins, followed by a second, third, and a not very pronounced fourth contraction. In this case no appreciable broadening of the channel is observed. The smallest diam-

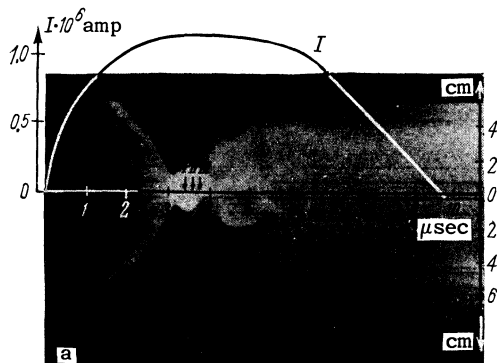


FIG. 9. a – photorecorder display with current oscillogram superimposed on it, b, c, d, – Kerr-cell records of the discharge. Pressure is 10 mm of Hg.



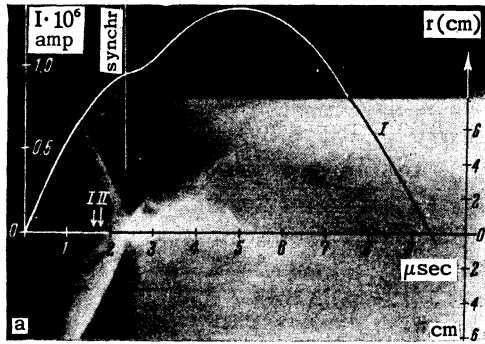
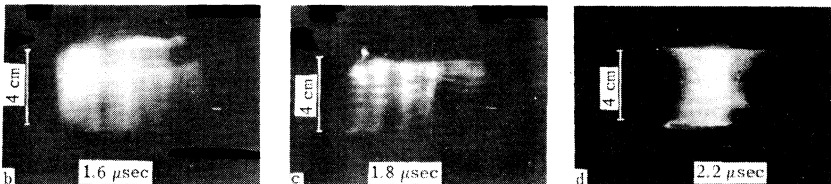


FIG. 10. a – photorecorder display with current oscillogram superimposed on it, b, c, d – Kerr-cell records of the discharge. Pressure is 1 mm of Hg.



eter of the “pinch” during the second and the third contraction is 2.0 cm, and the total length of time during which it lasts is  $2.4 \mu\text{sec}$ . Just as in the case of the short chambers, the expansion of the gas is accompanied by the separation of the gas into layers. The first two contractions occur at the same value of the current equal to  $1.04 \times 10^6$  amp, while the third and the fourth contractions correspond to currents of  $1.1 \times 10^6$  and  $1.3 \times 10^6$  amp.

(d) **Neutron measurements.** Neutron measurements were made by means of a counter and an apparatus of type B, and also by means of a scintillation counter. The thresholds of sensitivity of the apparatus were  $10^6$  and  $10^4$  neutrons respectively. The apparatus did not record any neutron emission.

#### 4. DISCUSSION OF RESULTS

(a) **Initial processes.** The discharge in the chamber during the time when its conductivity is small (Townsend build-up) occupies the whole volume, or its greater part. When short voltage pulses of  $0.1 \mu\text{sec}$  duration are applied to the chamber, diffuse streamers are observed which spread over the whole volume of the chamber. When the conductivity increases and the current in the discharge attains values of tens of kiloamperes, the skin effect becomes distinctly evident. The start occurs after the formation of the conducting layer situated along the periphery of the chamber. As we have seen, its thickness does not vary appreciably at pressures of 10 and 1 mm of Hg (Fig. 11), and only at a pressure of 0.1 mm of Hg does it become appreciably less. The varia-

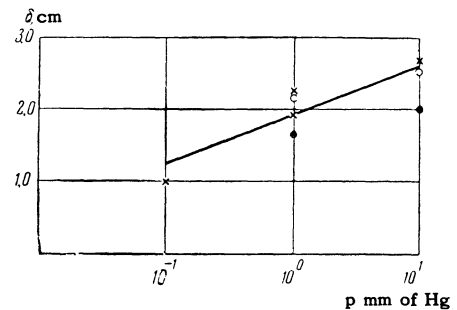


FIG. 11. Variation of the thickness of the conducting layer with pressure: O – large chamber, x – small chamber, ● – chamber with conical electrodes.

tion in the current at which the break-away occurs is shown in Fig. 12 as a function of the pressure.

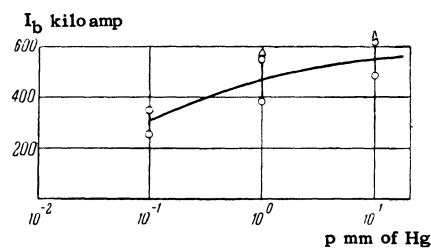


FIG. 12. Break-away currents at different pressures. Measured values: O – for small chambers, Δ – for large chambers.

The average conductivity  $\sigma$  in the luminous layer at the moment of the start can be roughly estimated from the thickness  $\delta$  of the layer (it may exceed the thickness of the skin-layer by a factor of 2 to 3). From the well known expression:

$$\sigma = c^2 t / 2\pi \delta^2 = (0.5 \div 1.4) \cdot 10^{14} \text{ CGS esu.}$$

The order of magnitude of this quantity may also be found from the longitudinal field strength  $E_R$  in the discharge at the instant of the start, on the assumption that the current in the layer is dis-

tributed uniformly:

$$\sigma = I_0 / 2\pi R \delta E_R,$$

where  $R$  is the radius of the chamber, and  $I_0$  is the current at the time it breaks away from the wall. By utilizing the measured values of  $I_0$  and  $E_R$  we obtain a conductivity of  $0.3 \times 10^{14}$ , which remains practically constant as the pressure is varied by two orders of magnitude. A gas which has such a conductivity has an electron temperature of 3 to 6 eV. The unavoidable evaporation of the walls leads to impurities in the deuterium which manifest themselves by the high luminosity of the gas after contraction, when the deuterium should be highly ionized and less luminous. As may be seen from photographs, there is no continuous conducting layer at pressures of 1 to 10 mm of Hg. Instead there is a network of channels which have a relatively higher luminosity and consequently a higher current density. Since the magnetic pressure is given by  $P_M \approx iH$  ( $H$  is the magnetic field,  $i$  is the current density), the pressure experienced by these channels is greater, and they start first. A layer of ionized gas is left behind them. The current in it will grow as the gas moves in towards the center.

Efficient capture of neutral gas by means of the charge-exchange mechanism becomes possible from the moment when the converging channels coalesce into one continuous front. At a pressure of 10 mm of Hg, the formation of a continuous annular layer occurs at a radius of 45 mm. At smaller pressures the radius of capture is larger. However, complete capture does not occur even in the case of a continuous annular layer. This is particularly noticeable at a pressure of 0.1 mm of Hg, when there is observed a series of contraction waves, which are possible only in the presence of residual gas. Thus the number of particles which the conducting layer will "sweep" towards the center can in actual fact differ appreciably from the number of particles present in the chamber cross section.

(b) **Contraction and scattering.** The speed of contraction of plasma in the discharge varies from zero up to a certain maximum value. Its increase depends on the pressure, on the circuit parameters, on the shape of the electrodes, and on the instability of the contracting layer. It was noted earlier that at  $p = 10$  mm of Hg the speed of the gas at the point where constrictions are formed may exceed the average speed (temperature) of the gas during contraction by a factor of 3 (and the temperature by an order of magnitude). At the instant of complete contraction, a longitudinal

redistribution of the particle density may occur, owing to the existence of constrictions.

The maximum speeds in the three variants of chamber design described earlier differ from each other only very little. However, if one compares the maximum speeds of contraction obtained for chambers of equal diameter with flat electrodes used in various installations<sup>2,5</sup> the influence of such a parameter as  $U_0/L_{init}$  becomes noticeable.

Figure 13 shows the curves of  $v_{max} = f(p)$  for

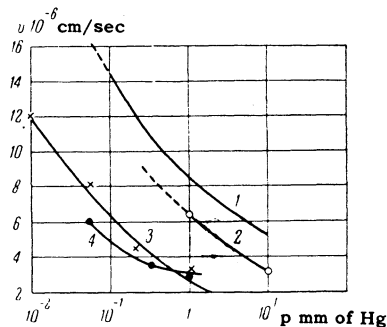


FIG. 13. Dependence of the maximum speed of contraction on the pressure for shock circuits with the parameter  $U_0/L_{init}$  having the values: 1 -  $1.4 \times 10^{12}$ ; 2 -  $0.7 \times 10^{12}$ ; 3 -  $2 \times 10^{11}$ ; 4 -  $5.7 \times 10^{10}$ .

apparatus with different values of  $U_0/L_{init}$ . The influence of the parameter  $U_0/L_{init}$  on the speed of contraction may be seen best of all in the case of  $p = 1$  mm of Hg. At this pressure the constrictions are least pronounced, and the errors in measuring the speeds of contraction are least. Even in the case of a relatively very rapid rate of rise of current, the converging layer of gas remains compact at a pressure of  $p = 1$  mm of Hg. At smaller pressures this compact nature is not preserved. As may be seen from Fig. 14,  $v_{max}$  grows mono-

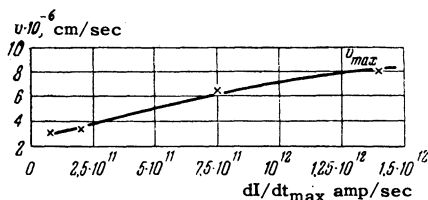


FIG. 14. Dependence of the maximum speed of contraction on the initial rate of current growth in the discharge;  $p = 1$  mm of Hg.

tonically, increasing by factor of 2.5 as  $U_0/L_{init}$  increases by a factor 10 [ $v_{max} \approx (U_0/L_{init})^{1/2.5}$ ].

At the instant of contraction, the current in the discharge depends significantly on the initial pressure. Figure 15 shows the measured and the calculated (cf. Leontovich and Osovets<sup>3</sup>) values of the current during the first contraction. The best agreement is observed at a pressure of 1 mm of Hg. At lower and, particularly, at higher pressures the discrepancies become appreciable. If one calculates the time of the first contraction by means of a formula given by Leontovich and Osovets<sup>3</sup> then the observed value always turns out to be higher than the calculated one. There are at least four reasons for such a discrepancy: (1) the

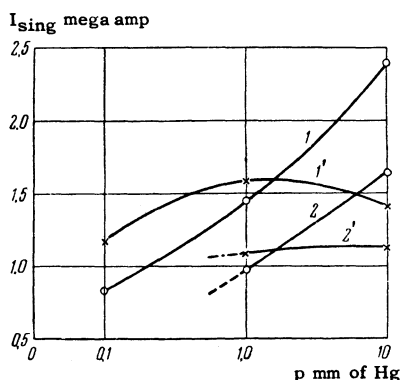


FIG. 15. Current in the discharge at the first contraction. 1, 1' - small chamber, 2, 2' - large chamber, O - calculated values, x - experiment.

deviation of the current from a linear form at times close to  $\tau_{sing}$  (which is important for large  $\tau_{sing}$  and large  $p$ ); (2) the smearing out of the current front and of the converging layer of gas; (3) the imperfect nature of the mechanism of "sweeping up" of the gas, owing to which only a portion and not the whole gas contained in the chamber is collected (this is more important at low pressures); (4) the capture of heavy particles from the chamber walls. A relatively satisfactory agreement between calculated and actual values is apparently explained by the fact that the various deviations compensate one another at least partially.

As we have seen, the contracting layer of gas, prior to colliding with the layers which it encounters, has a comparatively low ion and electron temperature, and therefore the degree of ionization in this layer must be relatively low (cf. also Lukianov and Sinitsyn<sup>6</sup>). The layer contains a large number of neutral particles. The principal part of the heating occurs during the short shock compression, when a part of the kinetic energy of directed motion of particles is transformed into heat. An evaluation of the temperature with the aid of formulas for the equilibrium state<sup>7</sup>  $T = I^2/4Nk$  is hardly justified in this case. It is therefore best to estimate the maximum temperature by utilizing  $v_{max}$  ( $v_{max}^2 = 3kT/M_D$ ). Figure 16 shows the temperature determined in this manner for small chambers at various pressures. The limiting

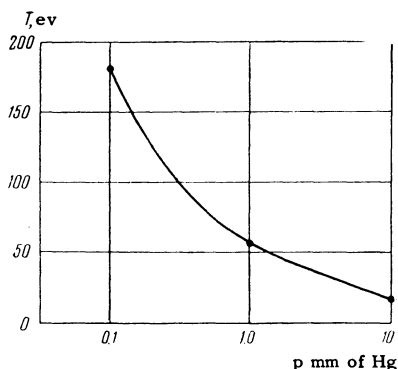


FIG. 16. Maximum gas temperature during contraction (small chamber).

temperature attained at a pressure of 0.1 mm of Hg amounts to 180 eV. One might think that under our conditions, neutrons of thermonuclear origin might be produced by the higher speed of contraction. However, a simple calculation shows that this is not the case. The neutron yield  $A$  may be estimated from the well-known relationship

$$A = \frac{1}{2} n N \langle \sigma V \rangle \tau l,$$

where  $n$  is the particle density in the column at the instant of compression,  $N$  is the initial number of particles in the cross section of the chamber,  $\langle \sigma V \rangle$  is the cross section for the reaction,  $l$  is the length of the column in cm,  $\tau$  is the time of contraction in sec. Calculations made on the basis of the following assumptions: (1) all the gas is captured during contraction, (2) the measured speed is the average speed for a Maxwellian distribution of particle velocities, (3)  $\tau = 10^{-6}$  sec, give a neutron yield of approximately  $10^3$  at  $p = 0.1$  mm of Hg. This value is below the threshold of sensitivity of the recording devices. At higher pressures the neutron yield is even less.

Thus in the case of small chambers, in spite of the higher speed of contraction compared with the large chambers described earlier by Artsimovich et al.,<sup>2</sup> the neutron yield is either entirely absent or is very small. This result confirms the point of view expressed at that time with respect to the non-thermonuclear origin of the neutron radiation then observed.

The figures quoted above for the limiting compression of the gas, calculated from the ratio of the cross sections of the chamber and of the pinch, are somewhat overestimated. At a pressure of 10 mm of Hg the radius of capture is in actual fact smaller than the diameter of the chamber. If the gas is collected in a column starting with the radius of capture, then the limiting compression amounts approximately to 10. If  $p = 0.1$  mm of Hg, it is impossible to introduce corrections because we have not one, but three compression waves. The most accurate result, apparently, is obtained at a pressure of 1 mm when the symmetry of contraction is well preserved, when a satisfactory agreement with results of calculation is observed, and when, probably, there is no appreciable smearing of the current front, as is indicated by the sharp boundaries of the pinch. The limiting compression in this case attains a value of 140. This number may be regarded only as a rough approximation, since we have no reliable estimate of the amount of captured gas.

During a shock compression of short duration one can observe inside the pinch simultaneous

movement of waves of compression and decompression moving towards each other. However, this is the only point of similarity with elementary wave processes.

The expanding front of the gas has a structure that differs sharply from a simple shock wave. The front oscillates several times, and for quite different reasons than those given by Leontovich and Osovets.<sup>3</sup> Some of the gas is directed towards the center and some continues its movement towards the boundaries of the chamber at a reduced speed. A relatively more luminous narrow channel is preserved at the center. It may be observed on photographs during several microseconds, until the current passes its maximum value. In the case of a simple shock compression, the gas would have remained at the center not longer than  $0.3 \mu \text{ sec}$ . It is natural to assume that at the center of the pinch the current continues to flow even after contraction, as was observed by means of probe measurements and at lower pressures and speeds of contraction.<sup>2,3</sup> The luminosity in the front of the expanding gas is due to neutral particles which are not held by the field of the current. As the current builds up in the boundary portions of the gas column, which have a certain amount of conductivity, the column breaks up into layers. The hottest particles are carried towards the center and give rise to repeated compressions, while the cold particles are directed towards the walls. After the walls have been bombarded, a conducting layer of heavy particles is formed there. The contraction of this layer proceeds at considerably lower speeds. At this time the current at the center falls, while the current at the walls rises.

The influence of electrodes on the development of the discharge should naturally be more pronounced in short chambers, owing to the shorter

time required for the metal vapor to penetrate deeply into the gap, and owing to the removal of heat by the electrodes. Both processes begin at the instant of onset of the discharge, but are most strongly pronounced after contraction. Before contraction, the temperature of the gas in the skin layer is not greater than 6 ev. The corresponding speed of neutral atoms of copper is equal to  $v_{\text{Cu}} = v_D \sqrt{M_D / M_{\text{Cu}}} = 2.3 \times 10^5 \text{ cm/sec}$ . Thus, the copper vapor will advance not more than 5 mm during contraction. An appreciable removal of heat at such speeds would be observed only after  $12 \mu \text{ sec}$ . After contraction (if  $p = 0.1 \text{ mm of Hg}$ ) the time for the removal of heat would amount to  $3.5 \mu \text{ sec}$ , while  $v_{\text{Cu}}$  would increase to  $2.8 \times 10^6 \text{ cm/sec}$ . It follows from these figures that it is not advantageous to conduct experiments with short chambers at lower pressures.

The author expresses his deep gratitude to Academician M. A. Leontovich and S. M. Osovets for valuable remarks.

<sup>1</sup>I. V. Kurchatov, *Атомная энергия* (Atomic Energy) **3**, 65 (1956).

<sup>2</sup>Artsimovich, Andrianov, Basilevskaja, Prokhorov, and Filippov, *Атомная энергия* (Atomic Energy) **3**, 84 (1956).

<sup>3</sup>M. A. Leontovich and S. M. Osovets, *Атомная энергия* (Atomic Energy) **3**, 81 (1956).

<sup>4</sup>V. S. Komel'kov and G. N. Aretov, *Dokl. Akad. Nauk S.S.S.R.* **110**, 559 (1956).

<sup>5</sup>Borzunov, Orlinskii and Osovets, *Атомная энергия* (Atomic Energy) **4**, 149 (1958).

<sup>6</sup>S. Iu. Lukianov and V. I. Sinitsyn, *Атомная энергия* (Atomic Energy) **3**, 88 (1956).

Translated by G. Volkoff